both the input and output coaxial lines at each frequency. These values were then used to remove the effect of the coaxial line from the measured amplifier data. The mean value of the effective coaxial line temperature when cooled in LN2 was 136 K and the standard deviation about the mean value over the frequency range was 36 K.

The accuracy of the noise temperature value calculated for the amplifier is dominated by the accuracy of the HP 8970S gain/noise measurement system. If this uncertainty is taken to be ± 0.25 dB, then the uncertainty in the amplifier noise is ± 30 K for the LN2 measurements and ± 80 K for the room-temperature measurements.

S parameters were measured with the two-chip amplifier at room and at LN2 temperature. These measurements utilized the previously described test setup in conjunction with a Wiltron 360 vector network analyzer. The room-temperature and cold (LN2) reflection, load, and transmission (through) calibrations were performed at the amplifier/stainless steel coax interface. The cold calibration was done with only the through adapter immersed in LN2 to avoid damaging the precision reflection and load elements. This has the effect of introducing an error in the phase reference plane owing to the uncalibrated change in the electrical length of the cold portion of the coaxial cable. The $S11$ and $S22$ magnitude is also in error because of the uncalibrated reduction in loss of the cold portion of the coax. The $S12$ and $S21$ magnitude is unaffected because the change in coax insertion loss is accounted for with the cold through calibration.

V. Experimental Results

When the noise contribution of the stainless steel coaxial cable on the input and output is removed from the measured data, the resulting amplifier noise generally shows a fourfold reduction between room temperature and LN2 operation over the 4 to 8 GHz range that was measured. This is in keeping with the expected scaling of MESFET amplifier noise with ambient temperature in Kelvin—in this case 77/300. As the data in Fig. 4 show, room-temperature amplifier noise ranges from 1000 to 1350 K from 4 to 6.5 GHz. The corresponding performance while operating in the LN2 bath ranges from 250 to 350 K. Above 6.5 GHz the improvement is less consistent with the predicted temperature scaling, but still shows a significant reduction: from 1250 to 1650 K down to 350 to 550 K.

The amplifier gain increased by several dB upon cooling, as shown by the S-parameter plots of Fig. 5. As described in Section IV, there is an uncertainty in the phase reference plane of the LN2 data. However, it is believed that this error is not more than 0.1%, as only about 3/4 in. of the 8 in. coaxial lines is submerged in LN2. The $S11$ and $S22$ data indicate a general expanding of the locus on the Smith chart upon cooling, but the center of these loci remains close to 50 Ω. It is believed that this effect is caused both by the uncalibrated reduction in loss of the cold portion of the stainless steel coax and by the increase in metallization conductivity of the MMIC inductors and on-chip traces when at the LN2 temperature. This latter effect, coupled with changes in the MESFET's, contributes to the observed increase in gain and reduction in noise temperature for LN2 operation.

VI. Conclusion

We have shown that GaAs MMIC devices can be packaged to operate at cryogenic temperatures and that operation at these temperatures can lead to enhanced noise performance. In particular, the generally observed scaling of noise temperature with ambient temperature (in Kelvin) for discrete GaAs MESFET amplifiers appears to also hold for GaAs MMIC amplifiers.

Modeling of GaAs MMIC cryogenic performance should be possible if noise parameter measurements of the MESFET are made at the temperature of interest. In the case of LN2 operation, this could be accomplished on a microwave wafer probe station if fitted with an appropriate cryogen container or cold plate. The resultant modeling capability should be useful in designing MMIC circuits to interface with high-temperature superconducting devices.

References

[1] S. Weinreb, "Low-noise, cooled GASFET amplifiers," *IEEE Trans. Microwave Theory Tech.*, vol MTT-28, pp. 1041–1054, Oct. 1980.
[2] M. W. Pospieszalski, S. Weinreb, R. D. Norrod, and R. Harris, "FET's and HEMT's at cryogenic temperatures—Their properties and use in low-noise amplifiers," *IEEE Trans. Microwave Theory Tech.*, vol. 36, pp. 552–560, Mar. 1988.
[3] D. Williams and T. Lum, Berkshire Technologies Inc., Oakland, CA 94609, private communication.

An Improved Version of the Almost Periodic Fourier Transform Algorithm with Applications in the Large-Signal Domain

J. Dreifuss, A. Madjar, and A. Bar-Lev

Abstract—**The almost periodic Fourier transform (APFT) algorithm is a useful tool in the analysis and design of nonlinear microwave circuits to which several large signals are applied simultaneously. It suffers, however, from a large spread in the calculated results. By combining the waveform balance (WB) approach with a modified form of the APFT algorithm, in which the number of randomly selected sampling points is increased, the overall computation accuracy is enhanced, the spread among results is reduced, and the computation time is practically unchanged. This modified approach is applied to the evaluation of large-signal S parameters of a MESFET and to the calculation of its 1 dB compression power, the intermodulation distortion (IMD) products, and the IP_3 points for a range of frequencies. The results are in excellent agreement with those parameters that are available from the manufacturer's measurements. The conversion gain of a MESFET mixer is also calculated and the reduced spread among the results is compared with that obtained by use of the original APFT algorithm.**

I. Introduction

The harmonic balance (HB) method has become a basic tool in modern analysis of such large-signal circuits as microwave networks employing nonlinear devices, for example power GaAs MESFET's [1], [2]. Recently, the HB method has also been used for the analysis of injection laser modulation problems [3]. The HB method overcomes the severe drawbacks of time-domain analysis, such as long transient periods that precede the steady state of interest, distributed-type circuit components which are difficult to model in the time domain, and circuits in which vastly different frequencies exist concurrently, for example, mixers. For all these cases the HB method today forms the best approach.

In the standard HB method [4] the network is divided into linear and nonlinear parts and the computation proceeds as

Manuscript received May 10, 1990; revised October 30, 1990.
The authors are with the Department of Electrical Engineering, Technion—Israel Institute of Technology, Haifa 32000, Israel.
IEEE Log Number 9041963

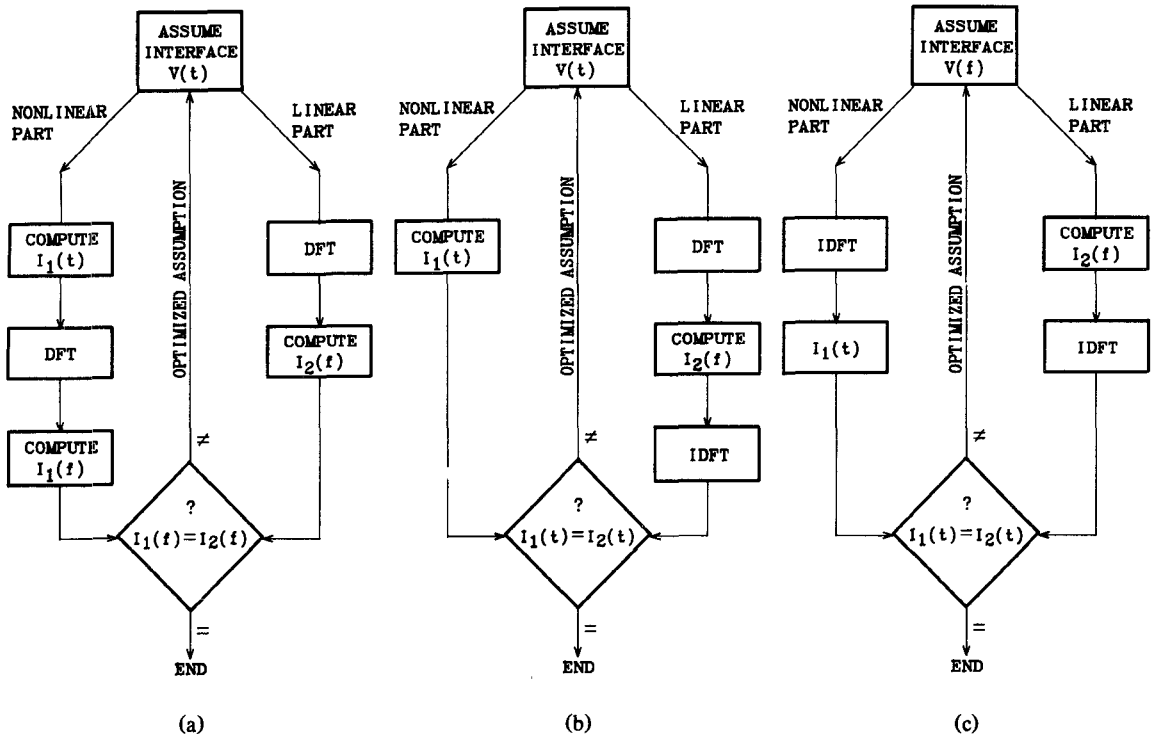

Fig. 1. · Computation schemes of (a) the HB method, (b) the WB method, and (c) the MWB method.

shown schematically in Fig. 1(a). A newer computation scheme, called the waveform balance (WB) technique [5], is similar to the HB method but the comparison of the computed interface currents into the linear and nonlinear parts is performed in the time domain, as shown in Fig. 1(b), thus replacing a DFT computing step with a IDFT one. The HB and WB methods, however, also have limitations. When several large-signal inputs are applied simultaneously to a circuit for which intermodulation, distortion, or saturation conditions are sought, difficulties arise. Since more than one large signal exists at the device ports and those signals are not harmonically related (though their frequencies are relatively close) the basic HB technique cannot be used. For such cases the modified harmonic balance (MHB) algorithm was developed [6]. This algorithm was used by us for treating large-signal microwave mixer properties [7] but its use constrains the nonlinear part of the device model to low Q values and the input frequencies to be multiples of the same fundamental frequency.

For cases in which multitone signals, of frequencies that are not harmonically related, are applied to nonlinear circuits a new Fourier transform algorithm has been published recently by Kundert *et al.* [8]. The signals are then defined as almost periodic and the algorithm is known as the almost periodic Fourier transform (APFT).

Such is the case of mixers where the exciting signals are harmonically unrelated and combination frequencies are generated owing to the strong nonlinearity. The combined signals then form an almost periodic function.

The APFT approach overcomes the above-mentioned limitations of the MHB method but suffers, in its turn, from a large spread in the calculated results. This is due to the random nature of the selected set of time points that are used for its computation. The method also requires the use of an inverse matrix routine, which is expensive in computing time and complexity and reduces the accuracy of the results.

The APFT algorithm as developed in [8] is adapted to the HB computing scheme. We show in this paper that a modified form of it, one that is simpler and shorter, can be developed based on another modification of the WB technique, called the MWB and shown schematically in Fig. 1(c). The MWB removes the necessity of a DFT step anywhere in the calculation process.

This paper describes an approach combining the modified forms of both the WB and APFT algorithms and therefore is called the MWB/APFT method. This new approach enhances the accuracy and reduces the spread among results of the same problem obtained in successive computing runs. The additional computing time required is small if it exists at all. This method is then used to evaluate intermodulation distortion and large-signal S parameters of a power MESFET. The calculated results are then compared with those measured by the manufacturer for various signal frequencies.

A second program based on the same modified method is used to obtain the nonlinear characteristics of a MESFET mixer, specifically its conversion gain, and a comparison is made of the spread of results obtained through use of the modified and basic APFT approaches.

II. The Modified WB/APFT Method

The first modification utilized here gets rid of the necessity of using the DFT algorithm and retains the use of the IDFT algorithm only. This reduces the computing time and enhances the accuracy. Unlike the HB and WB methods, the interface voltages are assumed in the frequency domain, as shown in Fig. 1(c). The linear part currents are calculated directly and then transformed by the IDFT to the time domain. The assumed voltages themselves are also transformed to the time domain by the IDFT algorithm to facilitate the calculation of the currents into the nonlinear part for comparison with the linear part ones. The APFT method necessitates first an IDFT step. When applied to the HB method of Fig. 1(a), a second DFT step is also necessary. With the MWB method of computation, following Fig. 1(c), the second DFT step is unnecessary, which saves an inverse matrix step. Although this operation is performed only once per set of frequencies, it forms the most time-consuming part of the APFT procedure. There is also an accuracy advan-

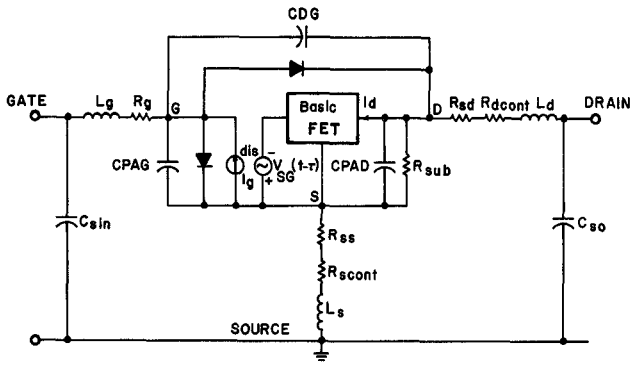

Fig. 2. The MESFET model network.

tage in that the round-off error caused by the matrix inversion involved is eliminated.

A second important modification is aimed at decreasing the condition number [8] of the handled matrices by increasing the number of the initial, randomly selected sampling time points (from which the final set of time points is chosen) above twice the Nyquist minimum, the number that was used in the original APFT algorithm [8]. That minimum, for N frequencies, is $2N+1$ points, corresponding to the number of coefficients to be found for the sine, cosine, and dc terms. By doubling that number to $2(2N+1)$ sampling points, a rectangular matrix of $[2(2N+1)]\times[2N+1]$ is formed. To obtain the currents in the nonlinear part, the matrix must first be orthogonalized to yield a square matrix for the next IDFT step. One then proceeds as in the original APFT method [8]. We found that by increasing the number of sampled time points to $5(2N+1)$, a much better orthogonalization can be obtained, which means that on successive runs of the program, each run based on a different choice from the random set of time points, a smaller spread is obtained among the results. The choice of $5(2N+1)$ approximately balances the additional computing time necessitated by the orthogonalization procedure with the time saved by no longer needing a matrix inversion procedure for obtaining the DFT.

III. Simulation Results

In order to evaluate the modified APFT and WB methods a computer program incorporating the modifications was written and applied to the analysis of the MESFET network of Fig. 2. An improved analytical ac large-signal model for the power MESFET [9] was utilized. The aim of the simulation was to obtain the large-signal S parameters and the IMD introduced by the nonlinearity of the active device. The MESFET chosen here was the HMF 1200 by Harris, which is a medium-power device whose electrical parameters are listed in [9]. The load impedance is assumed to be conjugately matched to the optimum load [11]. The power source is also conjugately matched to the input impedance as calculated for the optimum load.

The large-signal device S parameters were calculated for the bias point $V_{DS}=8$ V, $V_{GS}=-1.5$ V. The results, including a comparison at the small-signal level with values available from the manufacturer [10], are shown in Figs. 3 and 4 for three frequencies: 4, 6, and 11 GHz. Only those S parameters which are strongly affected by the large input signals are presented. These are the magnitude of S_{21} shown in Fig. 3 and the magnitude and phase of S_{22} shown in Fig. 4.

The S parameters were calculated using the method suggested in [12], in which two sinusoidal sources of frequencies f_1 and f_2 (slightly shifted from f_1) are applied simultaneously to the input and output ports. Since f_1 and f_2 are not harmonically related, the modified APFT algorithm was used for the calculations, which were performed for a wide dynamic range of

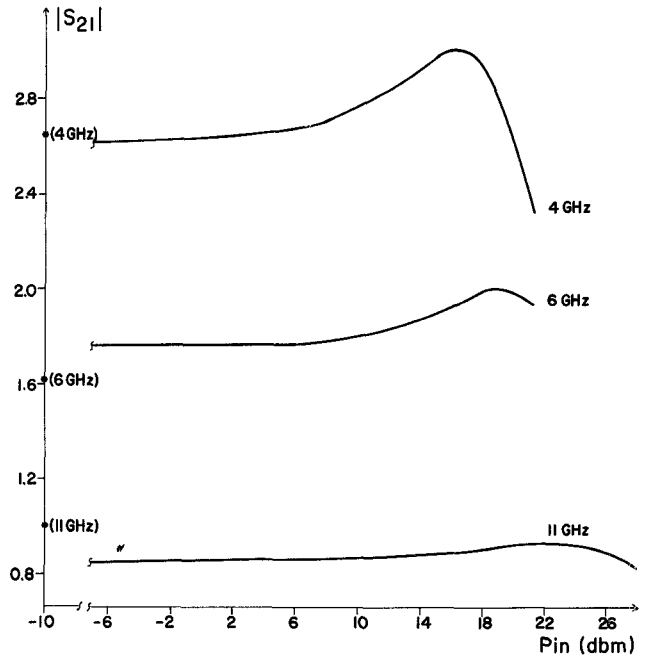

Fig. 3. Calculated large-signal $|S_{21}|$ for transistor HMF 1200 at 4, 6, and 11 GHz (the asterisk denotes manufacturer-supplied small-signal values).

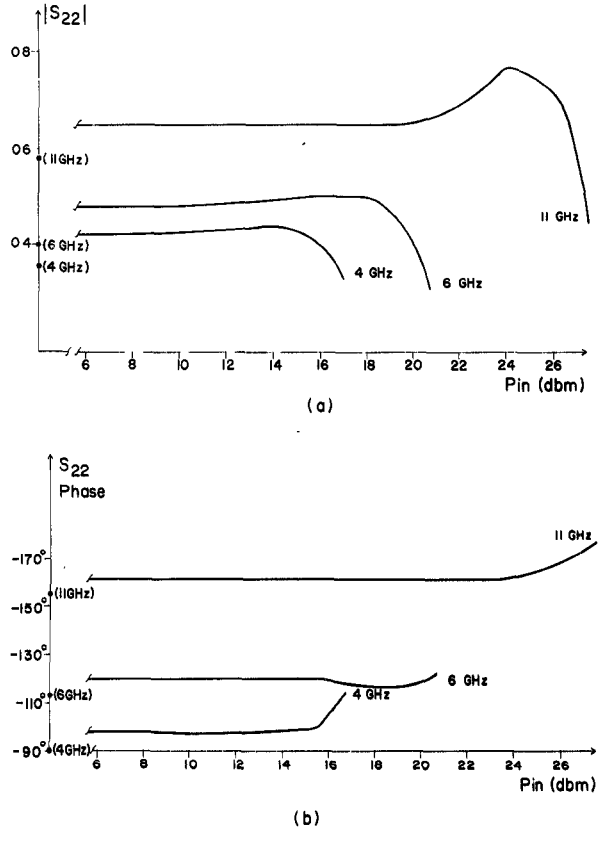

Fig. 4. Calculated large-signal (a) magnitude and (b) phase of S_{22} for transistor HMF 1200 at 4, 6, and 11 GHz (the asterisk denotes manufacturer-supplied small-signal values).

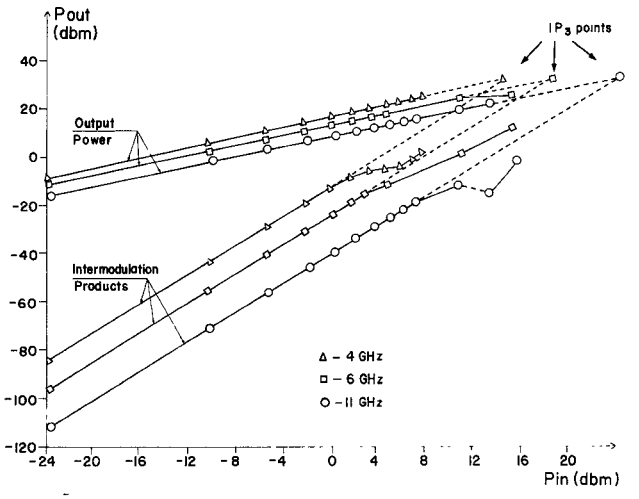

Fig. 5. Output power versus input power of fundamental and intermodulation products and the IP_3 points for the HMF 1200 MESFET at 4, 6, and 11 GHz.

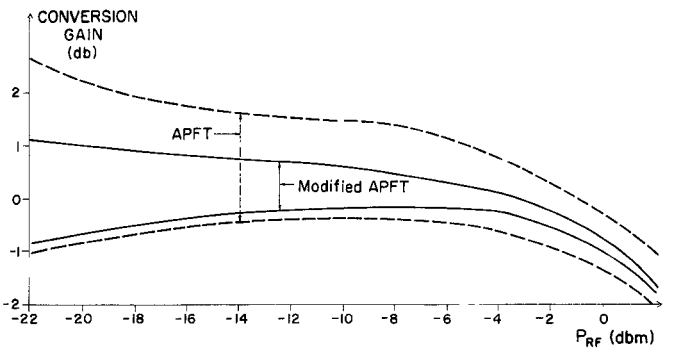

Fig. 6. Spread in results of conversion gain calculation for NE 710 MESFET mixer when using the APFT algorithm (----) or its modified form (———). Mixer data: $V_{DD} = 4$ V; $V_{GS} = -.75$ V; $f_{LO} = 12$ GHz; $f_{IF} = 0.5$ GHz; $P_{LO} = 2$ dBm.

TABLE 1
COMPARISON OF CALCULATED (a) AND MANUFACTURER-SUPPLIED (b) VALUES FOR GAIN AND POWER OUTPUT AT THE 1 dB COMPRESSION POINT AND THE INTERMODULATION INTERCEPT POINT IP_3 FOR MESFET HMF 1200 BY HARRIS

f [GHz]	$G_{1\,dB}$ [dB]		$P_{1\,dB}$ [dBm]		IP_3 [dBm]
	(a)	(b)	(a)	(b)	(a)
4	14.5	13.7	25	27.5	31
6	11.5	10.9	26	27.8	31.5
11	6.0	6.7	27	28.7	32

signal levels. The IMD values were calculated by the accepted two-tone method, with the two tones spaced 1 MHz apart and centered at the three center frequencies of 4, 6, and 11 GHz. In Fig. 5 the predicted P_{out} versus P_{in} is shown for the HMF 1200 device model together with the IMD products that result from its nonlinearities.

The simulations were performed for input power levels of up to $P_{in} = 8$ dBm for 4 GHz and 15.5 dBm for 6 and 11 GHz. At higher input powers the device enters deep saturation and the five fundamental harmonics used in our present program were no longer sufficient for accurate results. This is not a basic limitation of the modified method as a larger number of harmonics can be used at the expense of longer computing times. The intermodulation products of Fig. 5 show the three distinct regions that were described by Higgins and Kuvas [13]. For MESFET's formed by ion implantation, such as the HMF 1200, the IMD magnitude becomes proportional to the cube of the input signal level for large input powers.

The point at which the fundamental and IMD powers will tend to be equal at extreme input powers is marked on Fig. 5 and is known as the third-order intercept point (IP_3). It is, however, a purely theoretical concept. Table I summarizes the values of the output powers, P_{out} at the 1 dB compression points, the gains $G_{1\,dB}$ at those points, and the IP_3 input power values as obtained by the simulation and compares them to the values available from the manufacturer for the three frequencies used.

The agreement between the two sets of numbers is very good at all the frequencies, considering that the manufacturer's supplied numbers are only typical ones. It should also be noted that there is a good correlation between the input powers corresponding to the IP_3 points and the values of input powers at which the magnitudes of $|S_{21}|$ and $|S_{22}|$ begin to drop in Figs. 3 and 4.

A second simulation program, using the modified APFT method, was written for evaluating the conversion gain from the input RF signal to the output IF signal of a MESFET mixer. The device chosen in this case was an NE 710 by NEC, which is a low-noise device whose parameters are given in Table II. The analysis of mixers always involves signals which are harmonically unrelated and its simulation necessitates a high level of accuracy in the transform matrix evaluation since both very large and very small signals are present at the same time, as pointed out by Maas [14]. To illustrate the benefit of using a higher number of sampling points in our modified APFT algorithm, the spread in conversion gain results obtained by the original APFT approach is compared in Fig. 6 with that obtained by the modified method. The mixer which was simulated was a typical one, as described in a previous paper [15]. The spread in dB in the results of the APFT compared with that of the modified APFT is 1.6 times larger at -22 dB input level, 2.3 times larger at -10 dBm input level, and 4 times larger at 0 dBm input power level.

IV. CONCLUSIONS

Use of the MWB approach combined with a modified form of the APFT algorithm involving an increased number of time sampling points has been shown to result in a versatile simulation scheme for nonlinear microwave circuits. The modified method was applied to computing important design data such as large-signal S parameters, intermodulation products including IP_3 points, and 1 dB compression points, all with a high level of accuracy, as manifested by an excellent agreement with measured results. Application of the modified APFT approach to

TABLE II
MESFET NE710 DEVICE AND PACKAGE PARAMETERS

MESFET NE710 Device Parameters:		
1	Forward Conduction Voltage (VF)	0.50 V
2	Cutoff Voltage (VCUT)	0.80 V
3	VSG for Max GDS (VGDSM)	0.20 V
4	Built-in Potential (PHI)	0.80 V
5	Device Max Current (CURON)	56.0 mA
6	Device Current for VSG = 0 (CURDSS)	27.0 mA
7	Device Current for VSG = VGDSM (CURDSM)	13.5 mA
8	GM for VSG = 0 (GM0)	75.00 mmho
9	GD Value for VSG = VDS = 0 (GD00)	80.00 mmho
10	GD Value for VSG = VGDSM (GDSM)	4.00 mmho
11	CVSG Value for VSG = 0 (C0)	0.230 pF
12	GVDS Value for VDS = VSG = 0 (CM0)	0.0000 pF
13	(−DVSG) Value for Large VDS (CMAX)	0.0000 pF
14	DVDS Value for Large VDS (CH)	0.0300 pF
15	DVDS Value for VDS = 0 (CL)	0.0253 pF
16	GVDS Value for Large VDS (CK)	0.0000 pF
MESFET NE710 Package/Circuit Parameters:		
1	Source Inductance (L_s)	5.00E-02 nH
2	Gate Inductance (L_g)	6.00E-02 nH
3	Drain Inductance (L_d)	0.00E+00 nH
4	Parasitic Input Capacitance (C_{sin})	0.00E+00 pF
5	Parasitic Output Capacitance (C_{so})	0.00E+00 pF
6	Gate Pad Capacitance (CPAG)	8.60E−02 pF
7	Drain Pad Capacitance (CPAD)	2.30E−02 pF
8	Drain to Gate Pad Capacitance (CDG)	3.30E−02 pF
9	Gate Metallization Resistance (R_g)	0.855 Ω
10	Substrate Leakage Resistance (R_{sub})	1.00E+05 Ω
11	Source Metallization Resistance (R_{scont})	1.900 Ω
12	Drain Metallization Resistance (R_{dcont})	1.900 Ω
13	Source Bulk Resistance (R_{ss})	0.000 Ω
14	Drain Bulk Resistance (R_{sd})	0.000 Ω
15	Channel Time Delay (τ)	2.400 ps

mixer simulation yields more accurate conversion gain results than are possible with the original APFT algorithm. The advantages of the modified method over the original one increase as the input power is increased, i.e. as the nonlinearities become more pronounced. Those advantages are achieved without materially changing the length of the computation times.

REFERENCES

[1] W. A. Curtice, "Nonlinear analysis of GaAs MESFET amplifiers, mixers and distributed amplifiers using the HB technique," *IEEE Trans. Microwave Theory Tech.* Vol. MTT-35, pp. 441–447, Apr. 1987.

[2] J. H. Haywood and Y. L. Chow, "Intermodulation distortion analysis using a frequency domain harmonic balance technique," *IEEE Trans. Microwave Theory Tech.* Vol. 36, pp. 1251–1257, Aug. 1988.

[3] S. Lezekiel, C. M. Snowden, and M. J. Howes, "HB model of laser diode," *Electron. Lett.*, vol. 25, no. 8, pp. 529–530, Apr. 1989.

[4] M. S. Nakhla and J. Vlach, "A piecewise HB technique for determination of periodic response of nonlinear systems," *IEEE Trans. Circuits Syst.* vol. CAS-23, pp. 85–91, Feb. 1976.

[5] V. D. Hwang and T. Itoh, "Waveform balance method for nonlinear MESFET amplifier simulation," *IEEE MTT-S Int. Microwave Symp. Dig.* 1989, pp. 581–584.

[6] R. Gilmore, "Nonlinear circuit design using the MHB algorithm," *IEEE Trans. Microwave Theory Tech.*, vol. MTT-34, pp. 1294–1307, Dec. 1986.

[7] J. Dreifuss, A. Madjar, and A. Bar-Lev, "A full large signal analysis of active microwave mixers," presented at 16th European Microwave Conf., Sept. 1986.

[8] S. Kundert *et al.*, "Applying HB to almost periodic circuits," *IEEE Trans. Microwave Theory Tech.*, Vol. 36, pp. 366–378, Feb. 1988.

[9] A. Madjar, "An improved analytical AC large signal model for the GaAs MESFET," *IEEE Trans. Microwave Theory Tech.*, vol. 37, pp. 1519–1522, Oct. 1989.

[10] Harris, "HMF-1200 Power GaAs FET," Product Data.

[11] Harris, Application Note 2: "Output Power Match for P_{1db} Power FET Chips," Feb. 1987.

[12] V. Rizzoli *et al.*, "General purpose HB analysis of nonlinear microwave circuits under multi tone excitation," *IEEE Trans. Microwave Theory Tech.* vol. 36, pp. 1650–1660, Dec. 1988.

[13] J. A. Higgins and R. L. Kuvas, "Analysis and improvement of inter modulation distortion in GaAs Power FETS." *IEEE Trans. Microwave Theory Tech.*, vol. MTT-28, pp. 9–17, Jan. 1980.

[14] S. A. Maas, "Two tone intermodulation in diode mixers," *IEEE Trans. Microwave Theory Tech.*, vol. MTT-35, pp. 307–314, Mar. 1987.

[15] J. Dreifuss, A. Madjar, and A. Bar-Lev, "A novel method for the analysis of microwave two-port active mixers," *IEEE Trans Microwave Theory Tech.*, vol. MTT-33, pp. 1241–1244, Nov. 1985.

High-Frequency Efficient Reflection Multiplier

K. Rauschenbach, C. A. Lee, and M. V. Schneider

Abstract—**We propose and calculate the performance of a new resistive balanced reflection multiplier capable of high-efficiency operation at submillimeter wavelengths, beyond the useful range of varactor-type multipliers. The multiplier and associated filters can be fabricated with monolithic thin-film techniques to sufficiently minimize high-frequency parasitic elements so that near ideal efficiencies can be realized. A closed-form distributed analysis is used to show that this reflection design can achieve a 6.7% third-harmonic conversion efficiency, an approximate 23% increase compared with an ideal resistive balanced transmission multiplier.**

I. INTRODUCTION

Resistive frequency multipliers are capable of higher frequencies of operation and wider bandwidths than state-of-the-art varactor diode multipliers [1], [2], which have an inherent frequency limitation caused by the saturation velocity of the neutral space-charge boundary. Resistive multipliers have several additional advantages which make them desirable for many applications requiring a local oscillator or a swept frequency source. They are very stable and easy to tune because their resistance provides enough loss to prevent parametric oscillation. Furthermore, a resistive balanced antiparallel diode configuration will inherently reject certain unwanted harmonics and will provide higher output power than single-diode multipliers [3]. Resistive frequency multipliers, however, are not widely used because they are significantly less efficient than varactor multipliers at lower frequencies [4]–[9]. The conversion efficiency for generating the nth harmonic of a resistive multiplier is fundamentally limited to $1/n^2$ [10]–[13]. In contrast, a lossless nonlinear capacitance can theoretically convert up to 100% of the available generated power into any single harmonic [14], [15]. Unfortunately, the usable nonlinearity of the transition capacitance diminishes at frequencies above 100 GHz because the velocity of the boundary of the space-charge layer cannot

Manuscript received December 8, 1989; revised September 24, 1990.

K. Rauschenbach is with the Lincoln Laboratory, Massachusetts Institute of Technology, Lexington, MA 02173.

C. A. Lee is with the Department of Electrical Engineering, Cornell University, Ithaca, NY.

M. V. Schneider is with AT&T Bell Laboratories, Crawford Hill Laboratories, Holmdel, NJ 07733.

IEEE Log Number 9041955.